BABAR-CONF-00/07
SLAC-PUB-8529

A measurement of the charged and neutral B meson lifetimes using fully reconstructed decays

The *BABAR* Collaboration

August 8, 2000

Abstract

Data collected with the *BABAR* detector at the PEP-II asymmetric B Factory at SLAC are used to study the lifetimes of the B^0 and B^+ mesons. The data sample consists of 7.4 fb^{-1} collected near the $\Upsilon(4S)$ resonance. B^0 and B^+ mesons are fully reconstructed in several exclusive hadronic decay modes to charm and charmonium final states. The B lifetimes are determined from the flight length difference between the two B mesons which are pair-produced in the $\Upsilon(4S)$ decay. The preliminary measurements of the lifetimes are

$$\begin{aligned} \tau_{B^0} &= 1.506 \pm 0.052 \text{ (stat)} \pm 0.029 \text{ (syst) ps}, \\ \tau_{B^+} &= 1.602 \pm 0.049 \text{ (stat)} \pm 0.035 \text{ (syst) ps} \end{aligned}$$

and of their ratio is

$$\tau_{B^+}/\tau_{B^0} = 1.065 \pm 0.044 \text{ (stat)} \pm 0.021 \text{ (syst)}.$$

Submitted to the XXXth International Conference on High Energy Physics, Osaka, Japan.

The *BABAR* Collaboration

B. Aubert, A. Boucham, D. Boutigny, I. De Bonis, J. Favier, J.-M. Gaillard, F. Galeazzi, A. Jeremie, Y. Karyotakis, J. P. Lees, P. Robbe, V. Tisserand, K. Zachariadou

Lab de Phys. des Particules, F-74941 Annecy-le-Vieux, CEDEX, France

A. Palano

Università di Bari, Dipartimento di Fisica and INFN, I-70126 Bari, Italy

G. P. Chen, J. C. Chen, N. D. Qi, G. Rong, P. Wang, Y. S. Zhu

Institute of High Energy Physics, Beijing 100039, China

G. Eigen, P. L. Reinertsen, B. Stugu

University of Bergen, Inst. of Physics, N-5007 Bergen, Norway

B. Abbott, G. S. Abrams, A. W. Borgland, A. B. Breon, D. N. Brown, J. Button-Shafer, R. N. Cahn, A. R. Clark, Q. Fan, M. S. Gill, S. J. Gowdy, Y. Groysman, R. G. Jacobsen, R. W. Kadel, J. Kadyk, L. T. Kerth, S. Kluth, J. F. Kral, C. Leclerc, M. E. Levi, T. Liu, G. Lynch, A. B. Meyer, M. Momayezi, P. J. Oddone, A. Perazzo, M. Pripstein, N. A. Roe, A. Romosan, M. T. Ronan, V. G. Shelkov, P. Strother, A. V. Telnov, W. A. Wenzel

Lawrence Berkeley National Lab, Berkeley, CA 94720, USA

P. G. Bright-Thomas, T. J. Champion, C. M. Hawkes, A. Kirk, S. W. O'Neale, A. T. Watson, N. K. Watson

University of Birmingham, Birmingham, B15 2TT, UK

T. Deppermann, H. Koch, J. Krug, M. Kunze, B. Lewandowski, K. Peters, H. Schmuecker, M. Steinke

Ruhr Universität Bochum, Inst. f. Experimentalphysik 1, D-44780 Bochum, Germany

J. C. Andress, N. Chevalier, P. J. Clark, N. Cottingham, N. De Groot, N. Dyce, B. Foster, A. Mass, J. D. McFall, D. Wallom, F. F. Wilson

University of Bristol, Bristol BS8 lTL, UK

K. Abe, C. Hearty, T. S. Mattison, J. A. McKenna, D. Thiessen

University of British Columbia, Vancouver, BC, Canada V6T 1Z1

B. Camanzi, A. K. McKemey, J. Tinslay

Brunel University, Uxbridge, Middlesex UB8 3PH, UK

V. E. Blinov, A. D. Bukin, D. A. Bukin, A. R. Buzykaev, M. S. Dubrovin, V. B. Golubev, V. N. Ivanchenko, A. A. Korol, E. A. Kravchenko, A. P. Onuchin, A. A. Salnikov, S. I. Serednyakov, Yu. I. Skovpen, A. N. Yushkov

Budker Institute of Nuclear Physics, Siberian Branch of Russian Academy of Science, Novosibirsk 630090, Russia

A. J. Lankford, M. Mandelkern, D. P. Stoker

University of California at Irvine, Irvine, CA 92697, USA

A. Ahsan, K. Arisaka, C. Buchanan, S. Chun

University of California at Los Angeles, Los Angeles, CA 90024, USA

J. G. Branson, R. Faccini,[1] D. B. MacFarlane, Sh. Rahatlou, G. Raven, V. Sharma

University of California at San Diego, La Jolla, CA 92093, USA

C. Campagnari, B. Dahmes, P. A. Hart, N. Kuznetsova, S. L. Levy, O. Long, A. Lu, J. D. Richman, W. Verkerke, M. Witherell, S. Yellin

University of California at Santa Barbara, Santa Barbara, CA 93106, USA

J. Beringer, D. E. Dorfan, A. Eisner, A. Frey, A. A. Grillo, M. Grothe, C. A. Heusch, R. P. Johnson, W. Kroeger, W. S. Lockman, T. Pulliam, H. Sadrozinski, T. Schalk, R. E. Schmitz, B. A. Schumm, A. Seiden, M. Turri, D. C. Williams

University of California at Santa Cruz, Institute for Particle Physics, Santa Cruz, CA 95064, USA

E. Chen, G. P. Dubois-Felsmann, A. Dvoretskii, D. G. Hitlin, Yu. G. Kolomensky, S. Metzler, J. Oyang, F. C. Porter, A. Ryd, A. Samuel, M. Weaver, S. Yang, R. Y. Zhu

California Institute of Technology, Pasadena, CA 91125, USA

R. Aleksan, G. De Domenico, A. de Lesquen, S. Emery, A. Gaidot, S. F. Ganzhur, G. Hamel de Monchenault, W. Kozanecki, M. Langer, G. W. London, B. Mayer, B. Serfass, G. Vasseur, C. Yeche, M. Zito

Centre d'Etudes Nucléaires, Saclay, F-91191 Gif-sur-Yvette, France

S. Devmal, T. L. Geld, S. Jayatilleke, S. M. Jayatilleke, G. Mancinelli, B. T. Meadows, M. D. Sokoloff

University of Cincinnati, Cincinnati, OH 45221, USA

J. Blouw, J. L. Harton, M. Krishnamurthy, A. Soffer, W. H. Toki, R. J. Wilson, J. Zhang

Colorado State University, Fort Collins, CO 80523, USA

S. Fahey, W. T. Ford, F. Gaede, D. R. Johnson, A. K. Michael, U. Nauenberg, A. Olivas, H. Park, P. Rankin, J. Roy, S. Sen, J. G. Smith, D. L. Wagner

University of Colorado, Boulder, CO 80309, USA

T. Brandt, J. Brose, G. Dahlinger, M. Dickopp, R. S. Dubitzky, M. L. Kocian, R. Müller-Pfefferkorn, K. R. Schubert, R. Schwierz, B. Spaan, L. Wilden

Technische Universität Dresden, Inst. f. Kern- u. Teilchenphysik, D-01062 Dresden, Germany

L. Behr, D. Bernard, G. R. Bonneaud, F. Brochard, J. Cohen-Tanugi, S. Ferrag, E. Roussot, C. Thiebaux, G. Vasileiadis, M. Verderi

Ecole Polytechnique, Lab de Physique Nucléaire H. E., F-91128 Palaiseau, France

A. Anjomshoaa, R. Bernet, F. Di Lodovico, F. Muheim, S. Playfer, J. E. Swain

University of Edinburgh, Edinburgh EH9 3JZ, UK

C. Bozzi, S. Dittongo, M. Folegani, L. Piemontese

Università di Ferrara, Dipartimento di Fisica and INFN, I-44100 Ferrara, Italy

E. Treadwell

Florida A&M University, Tallahassee, FL 32307, USA

[1]Jointly appointed with Università di Roma La Sapienza, Dipartimento di Fisica and INFN, I-00185 Roma, Italy

R. Baldini-Ferroli, A. Calcaterra, R. de Sangro, D. Falciai, G. Finocchiaro, P. Patteri, I. M. Peruzzi,[2] M. Piccolo, A. Zallo

Laboratori Nazionali di Frascati dell'INFN, I-00044 Frascati, Italy

S. Bagnasco, A. Buzzo, R. Contri, G. Crosetti, P. Fabbricatore, S. Farinon, M. Lo Vetere, M. Macri, M. R. Monge, R. Musenich, R. Parodi, S. Passaggio, F. C. Pastore, C. Patrignani, M. G. Pia, C. Priano, E. Robutti, A. Santroni

Università di Genova, Dipartimento di Fisica and INFN, I-16146 Genova, Italy

J. Cochran, H. B. Crawley, P.-A. Fischer, J. Lamsa, W. T. Meyer, E. I. Rosenberg

Iowa State University, Ames, IA 50011-3160, USA

R. Bartoldus, T. Dignan, R. Hamilton, U. Mallik

University of Iowa, Iowa City, IA 52242, USA

C. Angelini, G. Batignani, S. Bettarini, M. Bondioli, M. Carpinelli, F. Forti, M. A. Giorgi, A. Lusiani, M. Morganti, E. Paoloni, M. Rama, G. Rizzo, F. Sandrelli, G. Simi, G. Triggiani

Università di Pisa, Scuola Normale Superiore, and INFN, I-56010 Pisa, Italy

M. Benkebil, G. Grosdidier, C. Hast, A. Hoecker, V. LePeltier, A. M. Lutz, S. Plaszczynski, M. H. Schune, S. Trincaz-Duvoid, A. Valassi, G. Wormser

LAL, F-91898 ORSAY Cedex, France

R. M. Bionta, V. Brigljević, O. Fackler, D. Fujino, D. J. Lange, M. Mugge, X. Shi, T. J. Wenaus, D. M. Wright, C. R. Wuest

Lawrence Livermore National Laboratory, Livermore, CA 94550, USA

M. Carroll, J. R. Fry, E. Gabathuler, R. Gamet, M. George, M. Kay, S. McMahon, T. R. McMahon, D. J. Payne, C. Touramanis

University of Liverpool, Liverpool L69 3BX, UK

M. L. Aspinwall, P. D. Dauncey, I. Eschrich, N. J. W. Gunawardane, R. Martin, J. A. Nash, P. Sanders, D. Smith

University of London, Imperial College, London, SW7 2BW, UK

D. E. Azzopardi, J. J. Back, P. Dixon, P. F. Harrison, P. B. Vidal, M. I. Williams

University of London, Queen Mary and Westfield College, London, E1 4NS, UK

G. Cowan, M. G. Green, A. Kurup, P. McGrath, I. Scott

University of London, Royal Holloway and Bedford New College, Egham, Surrey TW20 0EX, UK

D. Brown, C. L. Davis, Y. Li, J. Pavlovich, A. Trunov

University of Louisville, Louisville, KY 40292, USA

J. Allison, R. J. Barlow, J. T. Boyd, J. Fullwood, A. Khan, G. D. Lafferty, N. Savvas, E. T. Simopoulos, R. J. Thompson, J. H. Weatherall

University of Manchester, Manchester M13 9PL, UK

[2]Jointly appointed with Univ. di Perugia, I-06100 Perugia, Italy

C. Dallapiccola, A. Farbin, A. Jawahery, V. Lillard, J. Olsen, D. A. Roberts
University of Maryland, College Park, MD 20742, USA

B. Brau, R. Cowan, F. Taylor, R. K. Yamamoto
Massachusetts Institute of Technology, Lab for Nuclear Science, Cambridge, MA 02139, USA

G. Blaylock, K. T. Flood, S. S. Hertzbach, R. Kofler, C. S. Lin, S. Willocq, J. Wittlin
University of Massachusetts, Amherst, MA 01003, USA

P. Bloom, D. I. Britton, M. Milek, P. M. Patel, J. Trischuk
McGill University, Montreal, PQ, Canada H3A 2T8

F. Lanni, F. Palombo
Università di Milano, Dipartimento di Fisica and INFN, I-20133 Milano, Italy

J. M. Bauer, M. Booke, L. Cremaldi, R. Kroeger, J. Reidy, D. Sanders, D. J. Summers
University of Mississippi, University, MS 38677, USA

J. F. Arguin, J. P. Martin, J. Y. Nief, R. Seitz, P. Taras, A. Woch, V. Zacek
Université de Montreal, Lab. Rene J. A. Levesque, Montreal, QC, Canada, H3C 3J7

H. Nicholson, C. S. Sutton
Mount Holyoke College, South Hadley, MA 01075, USA

N. Cavallo, G. De Nardo, F. Fabozzi, C. Gatto, L. Lista, D. Piccolo, C. Sciacca
Università di Napoli Federico II, Dipartimento di Scienze Fisiche and INFN, I-80126 Napoli, Italy

M. Falbo
Northern Kentucky University, Highland Heights, KY 41076, USA

J. M. LoSecco
University of Notre Dame, Notre Dame, IN 46556, USA

J. R. G. Alsmiller, T. A. Gabriel, T. Handler
Oak Ridge National Laboratory, Oak Ridge, TN 37831, USA

F. Colecchia, F. Dal Corso, G. Michelon, M. Morandin, M. Posocco, R. Stroili, E. Torassa, C. Voci
Università di Padova, Dipartimento di Fisica and INFN, I-35131 Padova, Italy

M. Benayoun, H. Briand, J. Chauveau, P. David, C. De la Vaissière, L. Del Buono, O. Hamon, F. Le Diberder, Ph. Leruste, J. Lory, F. Martinez-Vidal, L. Roos, J. Stark, S. Versillé
Universités Paris VI et VII, Lab de Physique Nucléaire H. E., F-75252 Paris, Cedex 05, France

P. F. Manfredi, V. Re, V. Speziali
Università di Pavia, Dipartimento di Elettronica and INFN, I-27100 Pavia, Italy

E. D. Frank, L. Gladney, Q. H. Guo, J. H. Panetta
University of Pennsylvania, Philadelphia, PA 19104, USA

M. Haire, D. Judd, K. Paick, L. Turnbull, D. E. Wagoner
Prairie View A&M University, Prairie View, TX 77446, USA

J. Albert, C. Bula, M. H. Kelsey, C. Lu, K. T. McDonald, V. Miftakov, S. F. Schaffner, A. J. S. Smith, A. Tumanov, E. W. Varnes

Princeton University, Princeton, NJ 08544, USA

G. Cavoto, F. Ferrarotto, F. Ferroni, K. Fratini, E. Lamanna, E. Leonardi, M. A. Mazzoni, S. Morganti, G. Piredda, F. Safai Tehrani, M. Serra

Università di Roma La Sapienza, Dipartimento di Fisica and INFN, I-00185 Roma, Italy

R. Waldi

Universität Rostock, D-18051 Rostock, Germany

P. F. Jacques, M. Kalelkar, R. J. Plano

Rutgers University, New Brunswick, NJ 08903, USA

T. Adye, U. Egede, B. Franek, N. I. Geddes, G. P. Gopal

Rutherford Appleton Laboratory, Chilton, Didcot, Oxon., OX11 0QX, UK

N. Copty, M. V. Purohit, F. X. Yumiceva

University of South Carolina, Columbia, SC 29208, USA

I. Adam, P. L. Anthony, F. Anulli, D. Aston, K. Baird, E. Bloom, A. M. Boyarski, F. Bulos, G. Calderini, M. R. Convery, D. P. Coupal, D. H. Coward, J. Dorfan, M. Doser, W. Dunwoodie, T. Glanzman, G. L. Godfrey, P. Grosso, J. L. Hewett, T. Himel, M. E. Huffer, W. R. Innes, C. P. Jessop, P. Kim, U. Langenegger, D. W. G. S. Leith, S. Luitz, V. Luth, H. L. Lynch, G. Manzin, H. Marsiske, S. Menke, R. Messner, K. C. Moffeit, M. Morii, R. Mount, D. R. Muller, C. P. O'Grady, P. Paolucci, S. Petrak, H. Quinn, B. N. Ratcliff, S. H. Robertson, L. S. Rochester, A. Roodman, T. Schietinger, R. H. Schindler, J. Schwiening, G. Sciolla, V. V. Serbo, A. Snyder, A. Soha, S. M. Spanier, A. Stahl, D. Su, M. K. Sullivan, M. Talby, H. A. Tanaka, J. Va'vra, S. R. Wagner, A. J. R. Weinstein, W. J. Wisniewski, C. C. Young

Stanford Linear Accelerator Center, Stanford, CA 94309, USA

P. R. Burchat, C. H. Cheng, D. Kirkby, T. I. Meyer, C. Roat

Stanford University, Stanford, CA 94305-4060, USA

A. De Silva, R. Henderson

TRIUMF, Vancouver, BC, Canada V6T 2A3

W. Bugg, H. Cohn, E. Hart, A. W. Weidemann

University of Tennessee, Knoxville, TN 37996, USA

T. Benninger, J. M. Izen, I. Kitayama, X. C. Lou, M. Turcotte

University of Texas at Dallas, Richardson, TX 75083, USA

F. Bianchi, M. Bona, B. Di Girolamo, D. Gamba, A. Smol, D. Zanin

Università di Torino, Dipartimento di Fisica Sperimentale and INFN, I-10125 Torino, Italy

L. Bosisio, G. Della Ricca, L. Lanceri, A. Pompili, P. Poropat, M. Prest, E. Vallazza, G. Vuagnin

Università di Trieste, Dipartimento di Fisica and INFN, I-34127 Trieste, Italy

R. S. Panvini

Vanderbilt University, Nashville, TN 37235, USA

C. M. Brown, P. D. Jackson, R. Kowalewski, J. M. Roney
University of Victoria, Victoria, BC, Canada V8W 3P6

H. R. Band, E. Charles, S. Dasu, P. Elmer, J. R. Johnson, J. Nielsen, W. Orejudos, Y. Pan, R. Prepost, I. J. Scott, J. Walsh, S. L. Wu, Z. Yu, H. Zobernig
University of Wisconsin, Madison, WI 53706, USA

1 Introduction

Precise measurements of the charged and neutral B meson lifetimes are needed for tests of theoretical models of heavy quark decays. An uncertainty of around 1% will be required to distinguish between models [1, 2] predicting different lifetime hierarchies among the B hadrons. The lifetimes are also required for other measurements and they provide a check of our understanding of the detector. The current world averages [3] for the B lifetimes are $\tau_{B^0} = 1.548 \pm 0.032\,\mathrm{ps}$ and $\tau_{B^+} = 1.653 \pm 0.028\,\mathrm{ps}$ and for their ratio is $\tau_{B^+}/\tau_{B^0} = 1.062 \pm 0.029$.

This paper presents preliminary measurements of the $B^\pm$ and $B^0/\overline{B}^0$ lifetimes and their ratio performed with data collected by the *BABAR* detector at the PEP-II asymmetric B Factory. At the $\Upsilon(4S)$, B mesons are produced in B^+B^- and $B^0\overline{B}^0$ pairs. In this analysis, one of the B mesons is fully reconstructed in a variety of clean hadronic two-body decay modes to charm and charmonium final states. An inclusive technique is used to reconstruct the decay vertex of the second B in an event, and the lifetimes are determined from the distance between the decay vertices of the two B mesons. This novel method, developed for use at an asymmetric B Factory, deals with event topologies similar to those addressed in the analyses of CP asymmetries where the time dependence is obtained from the distance between the two vertices. The measurement of B lifetimes using this technique is therefore a validation of the CP analyses. The systematic errors are quite different from previous measurements of the lifetimes and we expect substantial increases in the statistical precision in the future.

The paper is organized as follows. The method used to determine the B meson lifetimes is outlined in Section 2. The data sample and the detector components most relevant for this measurement are reviewed in Section 3. The event selection criteria and sample composition are described next in Section 4. The determination of the distance between the decay vertices of the two B mesons in a selected event is discussed in Section 5 together with the corresponding resolution function. The fitting procedure used to extract the B lifetimes from the neutral and charged B meson samples is described in Section 6. Systematic uncertainties are discussed in Section 7. The results are given at the end of the paper.

2 The decay length difference technique

The $\Upsilon(4S)$ decays exclusively into pairs of charged or neutral B mesons. At the PEP-II asymmetric B Factory the $\Upsilon(4S)$ decay products are Lorentz boosted ($\beta\gamma \approx 0.56$)[1] and travel far enough for their flight paths ($\approx 260\,\mu\mathrm{m}$) to be comparable to the experimental resolution ($\approx 150\,\mu\mathrm{m}$). Since no charged stable particles emerge from the $\Upsilon(4S)$ decay point, the production point of the B mesons is unknown and the B lifetimes have to be determined solely from their decay points. The difference between the decay lengths of the two B mesons in an event has been used for that purpose in this analysis.

Throughout the paper the signed quantity $\Delta z = z_{\mathrm{rec}} - z_{\mathrm{opp}}$ is used for the projection on the z axis (defined below) of the decay length difference between the fully reconstructed B meson, thereafter called B_{rec}, and the opposed B meson, B_{opp}. The event topology is sketched in Fig. 1, which is not drawn to scale. In the simplified situation where the B mesons are produced exactly at threshold and the $\Upsilon(4S)$ moves exactly along the z axis, $|\Delta z|$ is distributed exponentially with an average of $\langle|\Delta z|\rangle = (\beta\gamma)_B c\tau_B = (p_{\Upsilon(4S)}/m_{\Upsilon(4S)})c\tau_B$. Complications arise from several effects. The axis of the PEP-II beams is tilted by 20 mr with respect to the z axis, which is defined as

[1] The average boost of the center of mass frame is measured on a run-by-run basis using two-prong events [4].

parallel to the solenoidal magnetic field, and the energies of the beams fluctuate, giving the $\Upsilon(4S)$ momentum a Gaussian distribution with a standard deviation of 6 MeV/c. Furthermore, the energy release in the $\Upsilon(4\mathrm{S}) \to B\overline{B}$ decay makes the B mesons move in the $\Upsilon(4S)$ rest frame, resulting in a non-vanishing opening angle (smaller than 214 mr [5]) between the trajectories of the B mesons. The latter effect has the highest impact on the Δz distribution. In practice, all of these effects are small compared to the experimental resolution on Δz.

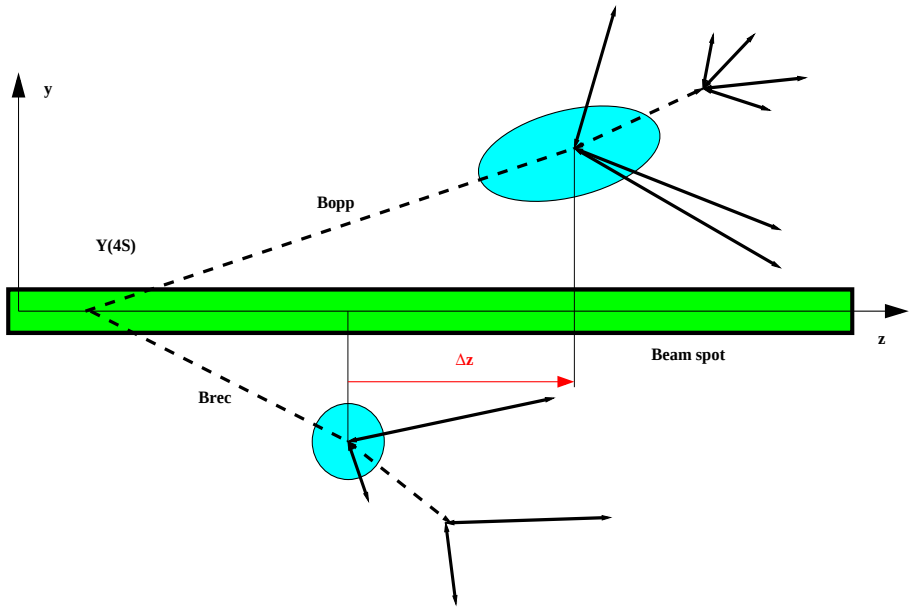

Figure 1: Event topology. The figure is not drawn to scale (see text).

3 The *BABAR* detector and data set

The data used in this analysis were collected by the *BABAR* detector at the PEP-II storage ring in the period from January to June, 2000. The total integrated luminosity of the data set is 7.4 fb^{-1} collected near the $\Upsilon(4S)$ resonance and 0.9 fb^{-1} collected 40 MeV below the resonance. The corresponding number of produced $B\overline{B}$ pairs is estimated to be 8.4×10^6.

The *BABAR* detector is described elsewhere [4]. For this measurement, the most important subdetectors are the silicon vertex tracker (SVT) and the central drift chamber (DCH), which jointly provide charged particle tracking, and the CsI electromagnetic calorimeter (EMC), from which photons and π^0s are reconstructed. The charged particle transverse momentum (p_T) resolution is approximately described by the formula $(\delta p_T/p_T)^2 = (0.0015\, p_T)^2 + (0.005)^2$, where p_T is in GeV/c. The SVT, with a typical single-hit resolution of 10 μm, provides vertex information in both the transverse plane and in z. The precision on charged particle momenta, neutral particle energies and spatial coordinates from the tracking and calorimetry leads to resolutions on invariant masses and other kinematical quantities which are adequate for a clean separation of the exclusive hadronic modes as described in Section 4. Impact parameter resolutions in the transverse and longitudinal coordinates are $\simeq 50\,\mu$m at high momentum, and better than 100 μm for $p_T > 0.6$ GeV/c. The achieved precision on exclusive and inclusive vertices are given in Section 5.

Particle identification is needed for complex decay modes and J/ψ reconstruction. Leptons and hadrons are identified using a combination of measurements from all *BABAR* components, including the $\mathrm{d}E/\mathrm{d}x$ energy loss using a truncated mean of 40 samples (maximum) in the DCH and 5 samples in the SVT. Electrons and photons are identified in the barrel and forward regions by the EMC. Muons are identified in the instrumented flux return (IFR). In the central polar angle region the Cherenkov ring imaging detector (DIRC) provides a separation better than three standard deviations between pions and kaons over the upper part of the momentum range of B decay products (above 700 MeV/c) where the $\mathrm{d}E/\mathrm{d}x$ sensitivity vanishes.

4 Event selection

B^0 and B^+ mesons are reconstructed in the following hadronic modes[2]; $B^0 \to D^{(*)-}\pi^+$, $D^{(*)-}\rho^+$, $D^{(*)-}a_1^+$, $J/\psi K^{*0}$ and $B^+ \to \overline{D}^{(*)0}\pi^+$, $J/\psi K^+$, $\psi(2S)K^+$. All final state particles are reconstructed. The selection criteria are devised to obtain final samples with approximately 90% purity and have been studied using the Monte Carlo simulation. Optimization for background rejection was performed using continuum data and sideband regions that do not contain signal events. The details of the selection of these events are described below.

4.1 Selection criteria

The basic objects used in the selection are charged tracks and neutral electromagnetic clusters. Charged tracks are built out of hits in the SVT and the DCH by a Kalman filter-based tracking algorithm [4]. To be retained, a track must not miss the average beamspot position by more than 1.5 cm in xy and 10 cm in z. Most tracks must penetrate halfway radially into the drift chamber (at least 20 hits are required) and have a momentum between 0.1 and 10 GeV/c. The latter restrictions do not apply to soft pions or low momentum tracks from a high multiplicity D decay. Electromagnetic clusters in the EMC are photon candidates when they carry more than 30 MeV, have a narrow transverse shower profile (the lateral moment defined in Ref. [4]) less than 0.8 and are not matched to a charged track.

The selection procedure begins by enforcing standard criteria [4] on the charged multiplicity, total energy, global event vertex position and event shape which enrich the sample with multihadronic events from $\Upsilon(4S)$ decays. A tight requirement on the normalized second Fox-Wolfram moment $R_2 (= H_2/H_0) < 0.5$ is applied in all analyses pertaining to this paper to reject jet-like events from the continuum.

The selection then proceeds by building a tree of composite objects (fast decaying particles) from tracks and photon candidates, culminating in a B candidate if one exists in the event. Geometrical fits are used to reconstruct decay points and declared successful when the χ^2 probability is above 0.1%. No goodness of fit requirement is enforced for the kinematic fits used to impose mass constraints.

Neutral pion candidates are formed from pairs of photon candidates with an invariant mass within 20 MeV/c^2 of the nominal π^0 mass and with a minimum energy of 200 MeV, except for those used in attempts to reconstruct a D^{*0}. A kinematic fit is performed on the selected candidates imposing the π^0 mass constraint.

K_S^0 candidates are reconstructed in the two charged pion decay mode only. Oppositely charged tracks are vertexed using a geometrical fit. The $\pi^+\pi^-$ invariant mass, computed at the vertex of the

[2]Throughout this paper, when a mode is quoted, its charge conjugate is implied.

two tracks, has to lie between 462 and 534 MeV/c^2. The opening angle between the flight direction and the K^0_S candidate momentum vector must be smaller than 200 mr. Finally, the transverse flight distance from the event primary vertex is required to be greater than 2 mm.

K and π meson candidates are combined to search for the following D meson decay modes; $D^0 \to K^-\pi^+$, $K^-\pi^+\pi^0$, $K^-\pi^+\pi^+\pi^-$, $K^0_S\pi^+\pi^-$ and $D^+ \to K^-\pi^+\pi^+$, $K^0_S\pi^+$. All kaons and the pions from two body modes are required to have a momentum above 200 MeV/c. This criterion is relaxed to 150 MeV/c for pions from three or four body final states. Candidates with an invariant mass within three standard deviations of the known mass are retained. The standard deviation computed event by event by the tracking algorithm was used after it was verified that the normalized error distribution (pull) was correctly estimated at the 10-20% level. The reconstruction of $D^0 \to K^-\pi^+\pi^0$ is restricted to the dominant resonant mode $D^0 \to K^-\rho^+$, $\rho^+ \to \pi^+\pi^0$. The $\pi^+\pi^0$ mass is required to lie within ± 150 MeV/c^2 of the known ρ mass and the ρ decay helicity angle in its rest frame, θ^*_ρ, is required to satisfy $|\cos\theta^*_\rho| > 0.4$. All D candidates must have a momentum greater than 1.3 GeV/c in the $\Upsilon(4S)$ frame and have a successful vertex fit. The accepted D candidates are mass constrained before they are used in subsequent intermediate state searches. Charged (neutral) D^* mesons are built by combining a D^0 with a soft charged (neutral) pion with momentum above 70 (100) MeV/c. Constraining the vertex of the D^{*+} to the beamspot vertical position within 40 μm improves the resolution on the soft pion direction and hence on Δm, the difference between the D^* and the D candidate invariant masses. This procedure has been verified to be bias-free in Monte Carlo events. An acceptable range of ± 3 standard deviations around the nominal Δm completes the D^* selection. The range limits (± 1.1 MeV/c^2 for $D^0 \to K^-\rho^+$, ± 0.8 MeV/c^2 for all other D^{*+} modes and ± 1.4 MeV/c^2 for the D^{*0}) are weighted averages of the standard deviations obtained from two-Gaussian fits to the experimental Δm distributions.

The charmonium meson selection is the same as that described in Ref. [6]. Leptonic decays of charmonium mesons are reconstructed from pairs of oppositely charged tracks considered either as electron or muon pairs. At least one decay product must be positively identified as a lepton. For an electron inside the EMC acceptance, this means a positive electromagnetic shower signature, otherwise that the measured $\mathrm{d}E/\mathrm{d}x$ be consistent with the electron hypothesis. For muon pairs, the second track has to be minimum ionizing in the EMC. In the electron case, when both tracks are inside the EMC acceptance and are such that $E/p > 0.5$, where E is the energy measured in the EMC and p is the momentum obtained from the tracking, bremsstrahlung photons found in the EMC are combined with the tracks to reconstruct the electrons prior to radiation. $J/\psi \to e^+e^-$ ($\mu^+\mu^-$) candidates must have an invariant mass between 2.95 (3.06) and 3.14 MeV/c^2. The invariant mass of the $\psi(2S) \to \mu^+\mu^-$ candidates is required to be within 50 MeV/c^2 of the known $\psi(2S)$ mass, but a less stringent lower limit of 200 MeV/c^2 is imposed for $\psi(2S) \to e^+e^-$ candidates. $\psi(2S) \to J/\psi\pi^+\pi^-$ decays are also reconstructed by combining oppositely charged pions with mass-constrained J/ψ candidates and selecting the $\psi(2S)$ invariant mass between 3.1 and 4.0 GeV/c^2 and the $\psi(2S) - J/\psi$ mass difference in a window of ± 15 MeV/c^2 around the nominal value.

B candidates are formed by combining a D^*, D, J/ψ or $\psi(2S)$ candidate with a π^+, ρ^+, a_1^+, K^{*0} or K^+ candidate having a minimum momentum of 500 MeV/c in the $\Upsilon(4S)$ frame. For $B^0 \to D^{(*)-}\rho^+$, the π^0 meson from the ρ^+ decay is required to have an energy higher than 300 MeV. For $B^0 \to D^{(*)-}a_1^+$, the a_1^+ meson, selected by combining three charged pions, must have an invariant mass between 1.0 and 1.6 MeV/c^2 and a successful vertex fit.

Kaon identification is used to reject background at the price of some loss in reconstruction efficiency. For most of the B^0 modes, a loose kaon selection, or no selection, is enough to reduce the background level to the required level. Tighter kaon identification is mandatory only for modes

with high combinatorial background, such as $B^0 \to D^- a_1^+$.

Finally, to achieve the required high signal to background ratio, stricter requirements on event shape variables are applied. A selection is performed on the angle, θ_T, between two thrust axes, namely the thrust axis computed from the tracks of the B meson candidate and the thrust axis of all the other charged tracks and neutral clusters in the event. A flat distribution is expected for B meson pairs while continuum events tend to peak at $\cos\theta_T = \pm 1$. For the $B \to D^*\rho$ modes, $|\cos\theta_T|$ is required to be less than 0.9 for the $D^0 \to K^-\pi^+$ and $K^-\pi^+\pi^0$ channels and less than 0.8 for $D^0 \to K^-\pi^+\pi^+\pi^-$ and $K^0_S\pi^+\pi^-$. The requirements are 0.8 and 0.7 for the $B^0 \to D^{*-}a_1^+$ modes and the same two couples of D modes. There is no restriction based on thrust for the $B \to D^{*-}\pi^+$ decays. For the B^0 decaying to charged D mesons, the requirements are 0.9, 0.8 and 0.7, if the D^- is accompanied by a π^+, a ρ^+ or an a_1^+. For the $B^- \to D^{(*)0}\pi^-$ decays, $|\cos\theta_T|$ is required to be less than 0.9 in the case of the $D^0 \to K^-\pi^+$ decay and to be less than 0.8 in all other cases. The requirement is 0.9 for the B decays to charmonium.

4.2 Sample composition

Signals for each decay mode in the selected sample are isolated by analyzing the two-dimensional distribution of the kinematical variables, ΔE and $m_{\rm ES}$, which have an intuitive meaning in the $\Upsilon(4S)$ rest frame. $\Delta E = E^*_{\rm rec} - E^*_b$ is the difference of the B candidate energy and the beam energy. $m_{\rm ES} = \sqrt{E^{*2}_b - \boldsymbol{p}^{*2}_{\rm rec}}$ is the mass of a particle with a reconstructed momentum $\boldsymbol{p}^*_{\rm rec} = \sum_i \boldsymbol{p}^*_i$ assumed to have the beam energy, as is the case for a true B meson. Candidates with $5.2 < m_{\rm ES} < 5.3\,{\rm MeV}/c^2$ and $|\Delta E| < 140\,{\rm MeV}$ are considered in further analyses. In case an event has several B candidates, only the one with the smallest ΔE is kept. The ΔE and $m_{\rm ES}$ variables are essentially uncorrelated. The resolution on $m_{\rm ES}$ is about $3\,{\rm MeV}/c^2$ and is dominated by the energy spread of the beams, inherent to the collider. The resolution on ΔE varies from mode to mode between 12 and 40 MeV. For each mode a rectangular signal region is defined by the three standard deviation bands in $m_{\rm ES}$ ($5.27 < m_{\rm ES} < 5.29\,{\rm GeV}/c^2$) and ΔE (an interval which depends on the mode).

For each mode, the sample composition was determined by fitting the $m_{\rm ES}$ distribution, for candidates within the signal region in ΔE, to the sum of a single Gaussian representing the signal and a background function used by the ARGUS collaboration [7]. The purity of each subsample is computed as the ratio of the area of the Gaussian in the $\pm 3\sigma$ range over the total area in this range. The results are summarized in Table 1. Figure 2 shows the $m_{\rm ES}$ distributions for the summed hadronic B^0 and B^+ modes with the fits superimposed.

To extract separately the B^0 and B^+ lifetimes, a thorough understanding of the background shape and composition is necessary. In the signal region, the background receives contributions from continuum, $B^0\overline{B}^0$ and B^+B^- pairs in various proportions for the different modes. A consistent background shape is found from studies of several samples; namely, on-resonance data events outside the signal region, off-resonance data, and generic $B\overline{B}$ and continuum Monte Carlo samples. The contamination of the B^+B^- subsamples by $B^0\overline{B}^0$ events, and vice versa, is found to be small.

5 Vertex reconstruction and resolution function

To extract the B meson lifetimes from the sample, the separate decay vertices have to be identified and the distance between them along the z axis, Δz, evaluated. The resolution function for Δz is the most critical ingredient of this analysis as the width of the Δz distribution is due to the combined effect of the B lifetime and the detector resolution.

Table 1: Two-body hadronic B^0 and B^+ decay candidate yields and signal purities from the fit to the $m_{\rm ES}$ distribution. Signal purities are estimated for $m_{\rm ES} > 5.27\,{\rm GeV}/c^2$.

Decay mode	Number of B candidates	Purity (%)
$B^0 \to D^{*-}\pi^+$	552±26	90
$B^0 \to D^{*-}\rho^+$	374±23	84
$B^0 \to D^{*-}a_1^+$	202±18	79
$B^0 \to D^-\pi^+$	537±25	90
$B^0 \to D^-\rho^+$	279±20	84
$B^0 \to D^-a_1^+$	194±18	73
$B^0 \to J/\psi\,K^{*0}$	167±15	90
$B^+ \to \overline{D}^0\pi^+$	1528±43	88
$B^+ \to \overline{D}^{*0}\pi^+$	446±25	89
$B^+ \to J/\psi,\psi(2S)K^+$	294±17	99
Total B^0	2210±58	86
Total B^+	2261±53	89

A geometric and kinematic fit of the fully reconstructed $B_{\rm rec}$ is performed and is required to converge. The masses of D and J/ψ resonances are fixed at the nominal values [3]. Furthermore, the vertices of short-living resonances are constrained to be identical to the B vertex. Two-Gaussian fits adequately describe the error distributions of the full Monte Carlo simulation used to model the signal events, with standard deviations ranging from 45 to 65 μm and normalized fluctuations (called pulls in the rest of the paper) around 1.1.

The vertex of the other B is determined via an inclusive and iterative procedure applied to all the tracks that are not associated with the $B_{\rm rec}$. To avoid biases from long-lived particles such as neutral strange particles decaying to two charged prongs (a topology known as a V^0 decay), as many V^0 decays as possible are reconstructed and subsequently treated as single tracks. A common vertex is then fitted using all tracks including the $B_{\rm opp}$ "pseudotrack" which is obtained from the $\Upsilon(4S)$ decay kinematics using the $B_{\rm rec}$ and the beamspot. The procedure is repeated, after removing tracks and V^0 decays which result in poor fits, until stability is achieved. The algorithm is highly efficient and successful in minimizing biases due to the secondary charm decays of the $B_{\rm opp}$. From the weighed means of two-Gaussian fits to Monte Carlo distributions of the residuals, one standard deviation errors of the order of 115 μm and biases around 25 μm are obtained. Although still present, the bias due to the charm particle lifetime is kept small.

With both vertices reconstructed, the decay length difference Δz is obtained. The Monte Carlo simulation was used to study the Δz resolution function $\mathcal{R}$ as a function of two variables, the residual $\delta(\Delta z) = (\Delta z)_{\rm rec} - (\Delta z)_{\rm generated}$ and the pull $\delta(\Delta z)/\sigma(\Delta z)$. Figure 3 presents the distributions for the decay $B^+ \to J/\psi\,K^+$. Two-Gaussian fits successfully describe the Monte Carlo residual and pull distributions. They give a one standard deviation width of $130 \pm 1\,\mu$m and a bias of $24.5 \pm 1\,\mu$m for the residual. The corresponding values for the pull are 1.21 ± 0.01 and 0.29 ± 0.01 respectively. As expected their widths are dominated by the $B_{\rm opp}$ vertex errors. Tails remain due to charm decays of the $B_{\rm opp}$. Because it is governed by the $B_{\rm opp}$ vertex, the resolution function shape is the same for all modes and also for neutral and charged B mesons. These comparisons are summarized in Table 2.

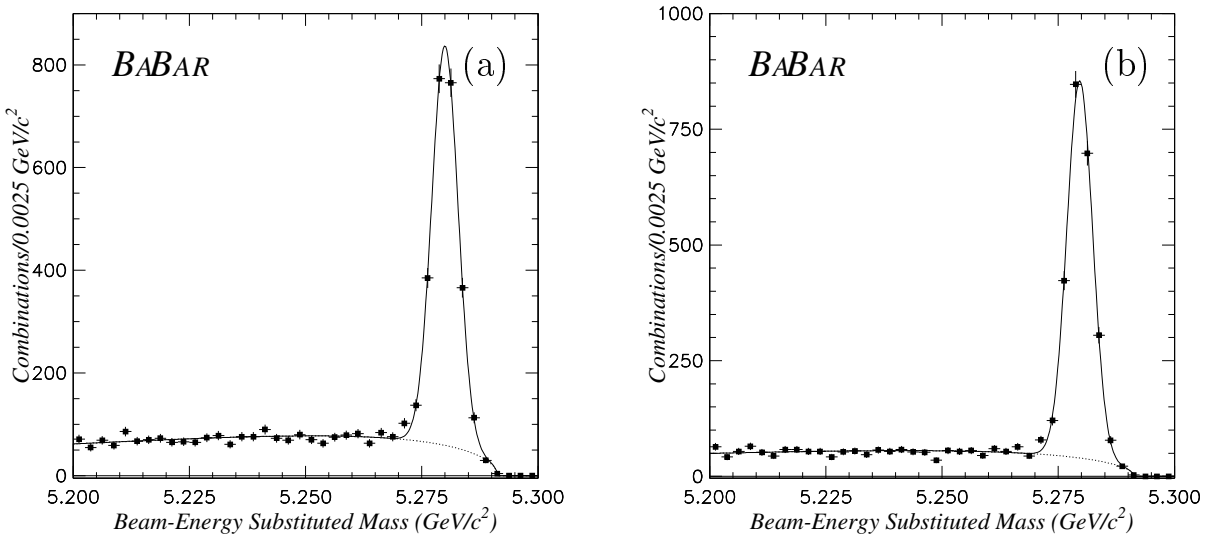

Figure 2: $m_{\rm ES}$ distribution for all the hadronic modes for (a) B^0 and (b) B^+. The signal is fitted to a Gaussian and for background we use the ARGUS parameterization [7]. The total numbers of signal events in all B^0 and B^+ modes are 2210 ± 58 and 2261 ± 53 respectively.

A common $\mathcal{R}$ function can be used for all modes. The shape of the resolution function can be fit with several parametrizations. Results for the pull representation (which is used in the likelihood function of the lifetime fit) are summarized in Table 3. It can be seen that a single Gaussian is too simple whereas a two-Gaussian line shape $G + G$ fits adequately. A fair agreement is also obtained with a function of the form $G + G \otimes E$, the sum of an unbiased Gaussian G and of the convolution of the same Gaussian with a decaying exponential E, as can be seen in Fig. 4.

Table 2: Parameters of the $G + G \otimes E$ resolution function $\mathcal{R}$ in the pull representation for a few B^0 and B^+ decay modes. The parameter g is the fraction of events in the pure Gaussian, s is the standard deviation of the Gaussian function and $\tau_{\rm r}$ is the decay constant of the exponential. A single $\mathcal{R}$ function for all modes is used in the lifetime fit.

	g	s	$\tau_{\rm r}$
$B^0 \to D^- \pi^+$	0.637 ± 0.031	1.019 ± 0.017	0.914 ± 0.062
$B^0 \to D^{*-} \pi^+$	0.666 ± 0.017	1.047 ± 0.010	1.024 ± 0.041
$B^+ \to J/\psi K^+$	0.678 ± 0.015	1.033 ± 0.008	0.956 ± 0.035
$B^+ \to \overline{D}^0 \pi^+$	0.644 ± 0.020	1.008 ± 0.010	0.833 ± 0.037

In a higher statistics Monte Carlo study, tails become apparent which cannot be reproduced by any of the parametrizations considered above. These "outlier" events in the tail are bound to bias the lifetime measurement if they are not accounted for in the fit. Some are due to long lived strange

Table 3: Values of the parameters for the different functional forms used to fit the Δz resolution function.

Parametrization	Parameters	χ^2/ndof
Single Gaussian (G)	mean = 0.273 $\pm$ 0.017 width = 1.148 $\pm$ 0.015	135.3/51
Gaussian centered at zero plus the same Gaussian convoluted with an exponential ($G + G \otimes E$)	g = 0.643 $\pm$ 0.029 s = 1.012 $\pm$ 0.0164 $\tau_{\rm r}$ = 0.936 $\pm$ 0.062	62.8/50
Two Gaussians ($G + G$)	f = 0.808 $\pm$ 0.047 s_1 = 0.998 $\pm$ 0.032 b_1 = 0.204 $\pm$ 0.025 s_2 = 1.931 $\pm$ 0.143 b_2 = 0.819 $\pm$ 0.139	40.0/48

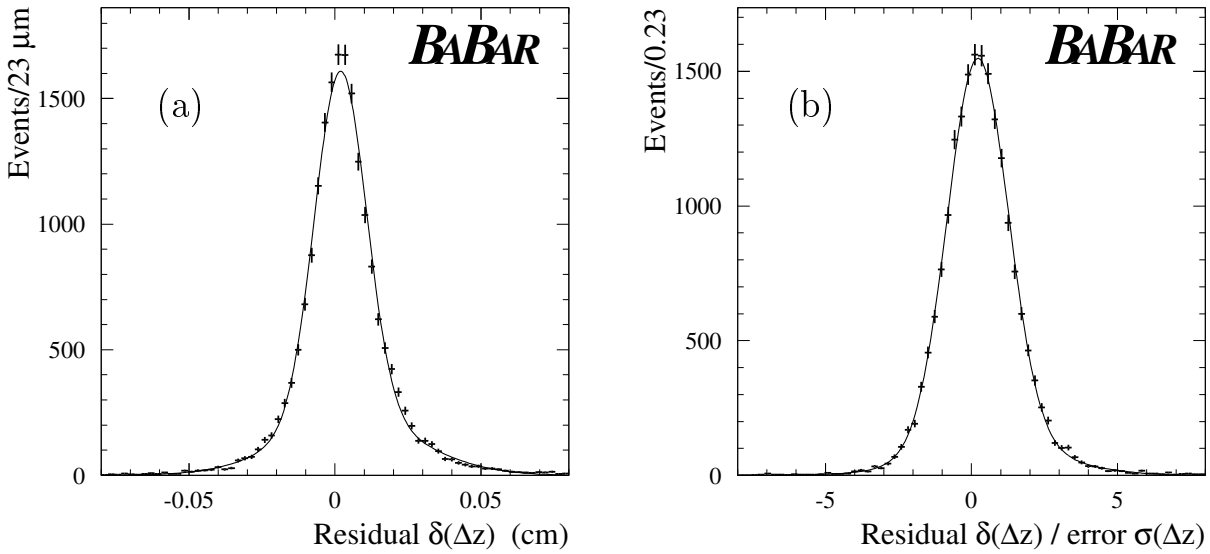

Figure 3: Distribution of (a) residual and (b) pull of Δz from a sample of $B^+ \to J/\psi K^+$ Monte Carlo simulated events.

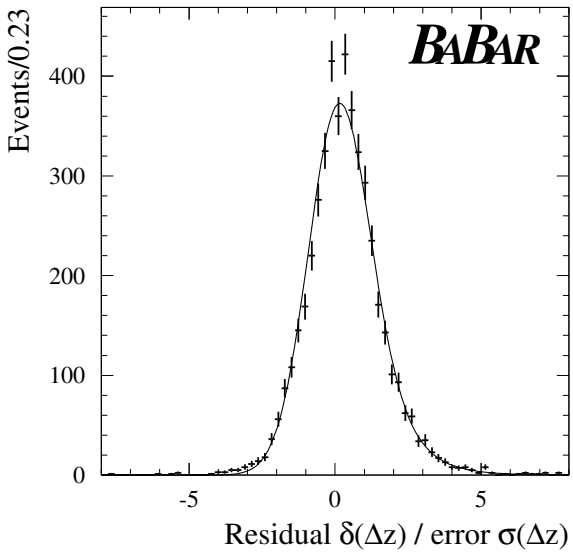

Figure 4: Fit of the Δz pull distribution on a sample of 5000 $B^0 \to D^-\pi^+$, $D^- \to K^+\pi^-\pi^-$ Monte Carlo simulated events, with a function consisting of a Gaussian centered at zero and the same Gaussian convoluted with an exponential ($G + G \otimes E$ parametrization).

particles forming a vertex with, e.g., the $B_{\rm opp}$ pseudotrack which is robust enough to survive the iterative vertex finding algorithm. To eliminate outliers, a requirement of a minimum of two real tracks to form the $B_{\rm opp}$ vertex, $|\Delta z| < 3000\,\mu$m and $\sigma(\Delta z) < 400\,\mu$m is imposed. There remain 1752 ± 46 (1879 ± 45) signal events in the neutral (charged) B lifetime samples after the selection.

The distribution of $\sigma(\Delta z)$ can be fitted to a Crystal Ball line shape function [8]. The fitted function is denoted $\rho(\sigma)$. Use of that spectrum with the pull representation of the resolution function provides an elegant way of implementing the lifetime fits as explained in Section 6.

Figure 5 shows the Δz distributions in the data for candidates satisfying $m_{\rm ES} > 5.27\,{\rm GeV}/c^2$. Superimposed are the Monte Carlo simulation predictions using the central values of the lifetimes of the B mesons from Ref. [3].

6 Lifetime fits

The B meson lifetimes are extracted from the Δz distributions of the selected events with an unbinned maximum likelihood fit. The measurements performed on each event i are represented by three input numbers: $(\Delta z)_i$, its error, σ_i, and $p_{{\rm sig},i}$. All events which satisfy $5.2 < m_{\rm ES} < 5.3\,{\rm GeV}/c^2$ and have ΔE in the signal region are input to the fit. $p_{{\rm sig},i}$ is the probability for an event i to come from signal. This probability is obtained from the independent fit of the $m_{\rm ES}$ spectrum using the ARGUS background function and a single Gaussian, as described previously (see Fig. 2). The fit determines the B lifetime, τ_B, the proportion of outliers, $p_{\rm out}$, and the two sets of parameters $\theta_{\rm resol}$ and $\theta_{\rm bkg}$ which describe the resolution function and the background shape, respectively.

The total probability density function (PDF) for an event i, $\mathcal{T}_i$, is the sum of three terms

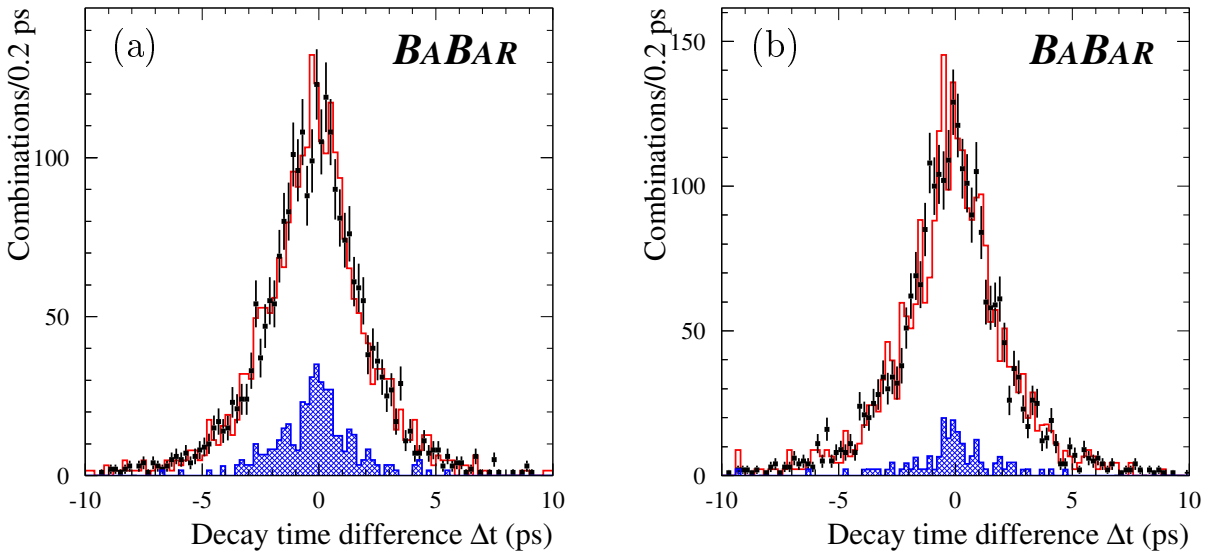

Figure 5: Comparison of Δt distributions in the data (points) and $B\overline{B}$ Monte Carlo events (solid line histogram) for (a) B^0 and (b) B^+. The contribution from the other type of $B\overline{B}$-decays in each case and from continuum events is also shown (hatched histogram). The simulation has been normalized to the data statistics.

describing the signal, the background and the outliers,

$$\mathcal{T}_i = \rho(\sigma_i) \times [p_{\mathrm{sig},i}\ \mathcal{S}((\Delta z)_i, \sigma_i; \tau_B, \theta_{\mathrm{resol}}) + (1 - p_{\mathrm{sig},i} - p_{\mathrm{out}})\ \mathcal{B}((\Delta z)_i; \theta_{\mathrm{bkg}}) + p_{\mathrm{out}}\ \mathcal{O}((\Delta z)_i)]\,.$$

The signal PDF, $\mathcal{S}$, is the result of a convolution of the theoretical Δz distribution (two exponential wings) and the pull representation of the Δz resolution function. Three or five resolution parameters, θ_{resol}, (depending on which parameterization is chosen for $\mathcal{R}$, $G+G$ or $G+G\otimes E$) are used to model the width and non-Gaussian tails. The parameters are free in the lifetime fit, i.e. the values of the parameters of the resolution function are extracted from the data themselves. Reducing the number of parameters modeling $\mathcal{R}$, which are unavoidably correlated to τ_B, has the effect of improving the statistical precision on the lifetime. The parameterization needs to be flexible enough to reproduce all features of the resolution function, however. The optimal choice depends on the statistics available.

The events in the substituted mass sideband carry most information on the background Δz distribution. A satisfactory description of this distribution is given by a function adding a single Gaussian and two independent exponential tails for the negative and positive Δz ranges. This parameterization uses six free parameters θ_{bkg}: the width and mean of the Gaussian, the "lifetimes" of the two exponentials and the fraction of events in each of the exponentials. Such a shape is flexible enough to account for the combinatorial background with continuum and $B\overline{B}$ contributions.

The outlier PDF, $\mathcal{O}$, is a single wide Gaussian with a fixed width of 2500 μm and a fixed mean of zero.

A full Monte Carlo sample with 5000 events in the channel $B^0 \to D^-\pi^+$, $D^- \to K^+\pi^-\pi^-$ was used to compare different parameterizations of the resolution function (see Table 3) which were

injected into signal-only lifetime fits. The $G+G$ model of the resolution function gives an unbiased result but the statistical error on the lifetime is increased by more than 50% compared to the case of a fixed $\mathcal{R}$. The single Gaussian model is both biased (overestimation of $\simeq 1.5\%$) and gives a 30% increase of the statistical error. The $G + G \otimes E$ is intermediate with a 0.3% overestimation of τ_B and the smallest increase of the statistical error (10%). With the present statistics, the $G + G \otimes E$ model of $\mathcal{R}$ lead to the smallest overall error. With high statistics, the $G + G$ model will become the optimum method.

To determine the B lifetimes, a combined fit to the Δz distributions of the B^0 and B^+ samples is performed. The two Δz distributions are not combined but are fitted simultaneously, with different sets of parameters (one per charge) to describe the lifetime, the background and the outliers. Since the resolution functions for neutral and charged B mesons are compatible, a single set of parameters is used to describe the resolution function for both samples. The result of the fit is

$$\begin{aligned} \tau_{B^0} &= 1.512 \pm 0.052 \text{ ps}, \\ \tau_{B^+} &= 1.608 \pm 0.049 \text{ ps}, \end{aligned}$$

where the errors are statistical only. The lifetime fit results are superimposed upon the B^0 and B^+ Δz distributions from the B reconstruction signal region in Figs. 6 and 7. The lifetime ratio is determined with a similar combined fit, this time to the B^0 lifetime and the ratio, which results in a value of

$$\tau_{B^+}/\tau_{B^0} = 1.065 \pm 0.044,$$

where, again, the error is statistical only. The final results after corrections described in the section on systematic errors are applied, are quoted in section 8.

7 Systematic uncertainties

The systematic errors associated with event selection, Δz measurement and lifetime fitting are discussed in turn.

It has been verified, using the B^0 and B^+ Monte Carlo samples, that the event selection does not distort the generated Δz distribution so that the lifetime measured from these samples is consistent with the input value. These checks are done with a limited number of simulated events which results in a statistical error on the lifetimes extracted from the fit. This Monte Carlo statistical error of 1.0% for B^0 and 0.9% for B^+ is taken as a systematic error on the lifetime measurements, labeled as "MC statistics" in Table 4.

The Δz resolution function $\mathcal{R}$ is a key ingredient of the lifetime measurements. The parameters describing $\mathcal{R}$ are results of the fit. Since they are correlated with the lifetime, part of the systematic error which comes from their uncertainty is transferred into the statistical error on the lifetime. This effect is estimated to be about 2%. For the systematic error associated with the resolution function modeling, two contributions are quoted. One is the difference between lifetimes obtained with fits using the $G + G$ and $G + G \otimes E$ parametrizations, a 0.3% effect. The other, at the level of 0.3% as well, is an overestimation of the distortion which may result from the simplifying assumption that a unique resolution function is suitable for all the modes.

The sensitivity of the lifetime measurement to quantities which enter into the determination of the $B_{\rm opp}$ vertex, namely the beam spot position and vertical size, and the $B_{\rm rec}$ momentum vector has been found to be negligible.

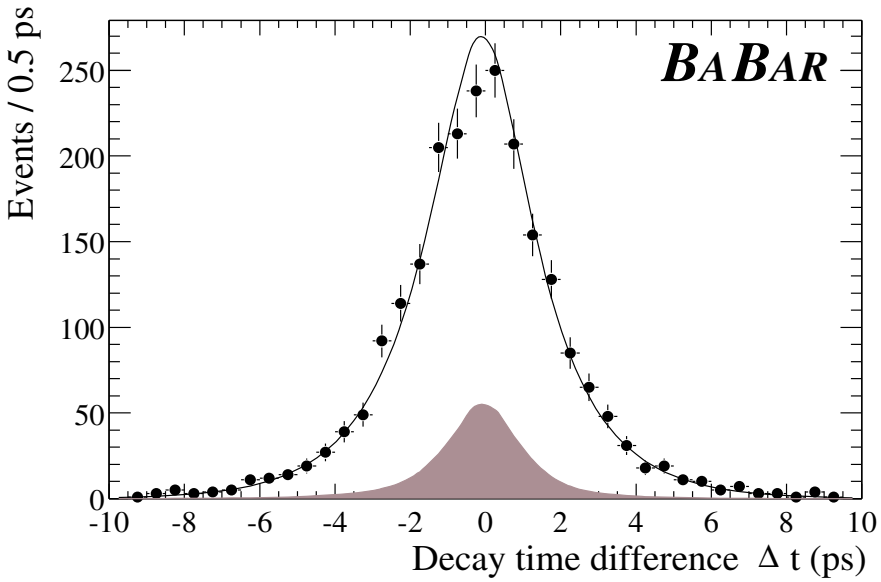

Figure 6: Δt distribution for $B^0/\overline{B}^0$ candidates in the signal region. The result of the lifetime fit is superimposed. The background is shown by the hatched distribution.

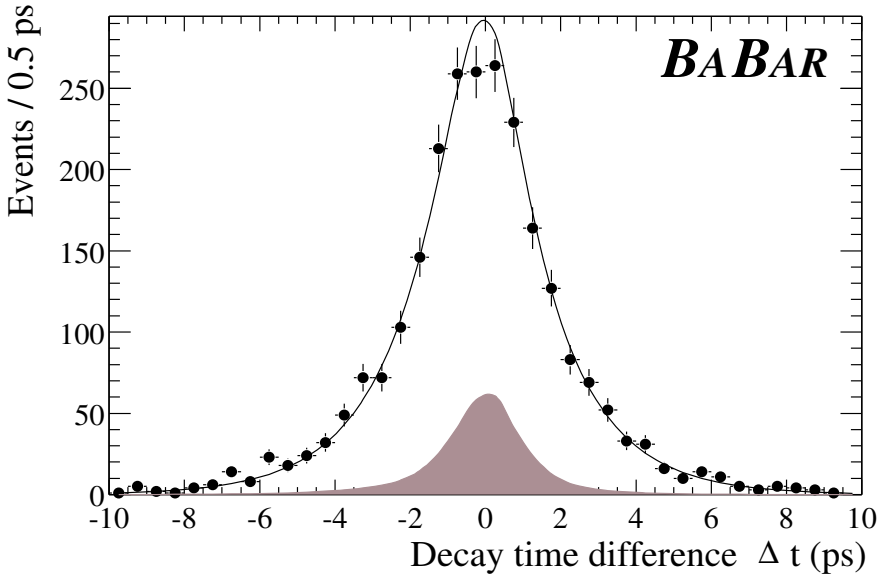

Figure 7: Δz distribution for $B^{\pm}$ candidates in the signal region. The result of the lifetime fit is superimposed. The background is shown by the hatched distribution.

The fit accounts for outlier events via a wide Gaussian function with fixed mean and width. Increasing the width from 2500 to 4000 μm gives a change of 1.1% (1.3%) to the B^0 (B^+) lifetimes. A change of 1000 μm in the mean gives an effect smaller by a factor three.

The effects of the detector geometry and alignment have been studied. These are smaller than the effects due to the charm lifetimes, and both parameterizations of the resolution function are flexible enough to accommodate small changes in the detector response. The associated systematic errors are included in those given for the resolution function model.

An overestimation of the uncertainty on the length scale measured along z has been obtained in considering the mechanical integrity of the SVT. A systematic error of 1% is assumed. Actual measurements of the length of the beam pipe with tracks are in progress and should considerably reduce this contribution to the error.

Systematic effects due to the boost enter due to the approximation of using the $\Upsilon(4S)$ boost for both B mesons in an event, as well as measurement error on the boost itself. The effect of the approximation is estimated to be a 0.4% shift and the measurement error from two-prong events is 0.3%. The central values for the lifetimes obtained from the fit are corrected for this shift and a conservative error of 0.4% is assigned. Adding the two contributions in quadrature, the systematic error due to the boost effects is 0.5%.

The systematic error due to the signal probability, $p_{\rm sig}$, is obtained by propagating the one standard deviation errors on the parameters of the line shape function to the lifetime. A 0.2% uncertainty is obtained.

The uncertainty in modeling the background is estimated by comparing the Monte Carlo distributions for the background in the signal region with the $m_{\rm ES}$ sideband, and also comparing $m_{\rm ES}$ sidebands in data and Monte Carlo simulation. The disagreement is more pronounced for B^+ mesons (1.1%) than for B^0 mesons (0.4%).

The stability of the results has been checked by splitting the data sample into subsamples of different $B_{\rm rec}$ modes and different times of data taking. A summary of all systematic errors as well as their sum in quadrature is given in Table 4.

Table 4: Summary of the systematic errors for the B lifetime measurements.

systematic effect	$\delta(\tau_{B^0})$ (fs)	$\delta(\tau_{B^+})$ (fs)	$\delta(\tau_{B^+}/\tau_{B^0})$	comment
MC statistics	16	14	0.014	
Parameterisation of resolution function $\mathcal{R}$	5	5	0.001	some included in the statistical error, see text
One single resolution function	5	5	0.008	
Beamspot, $p_{B_{\rm rec}}$	-	-	-	
Δz outliers	16	20	0.005	
Geometry and alignment	-	-	-	included in $\mathcal{R}$
z scale	15	16	-	cancels in ratio
Boost	6	6	-	cancels in ratio
Signal probability	3	2	0.005	
Background modeling	5	17	0.011	
Total in quadrature	29	35	0.021	

8 Summary

The preliminary results for the B meson lifetimes are

$$\begin{aligned} \tau_{B^0} &= 1.506 \pm 0.052 \text{ (stat)} \pm 0.029 \text{ (syst) ps}, \\ \tau_{B^+} &= 1.602 \pm 0.049 \text{ (stat)} \pm 0.035 \text{ (syst) ps} \end{aligned}$$

and for their ratio is

$$\tau_{B^+}/\tau_{B^0} = 1.065 \pm 0.044 \text{ (stat)} \pm 0.021 \text{ (syst)}.$$

These results are consistent with previous B lifetime measurements [3] and competitive with the most precise ones. The statistical errors dominate the uncertainties, while the systematic uncertainty on the lifetime ratio is smaller than the overall error of the world average for this quantity. There are ways to reduce some contributions; however, to reach a 1% total error on the B lifetime ratio remains a challenge.

9 Acknowledgments

We are grateful for the contributions of our PEP-II colleagues in achieving the excellent luminosity and machine conditions that have made this work possible. We acknowledge support from the Natural Sciences and Engineering Research Council (Canada), Institute of High Energy Physics (China), Commissariat à l'Energie Atomique and Institut National de Physique Nucléaire et de Physique des Particules (France), Bundesministerium für Bildung und Forschung (Germany), Istituto Nazionale di Fisica Nucleare (Italy), The Research Council of Norway, Ministry of Science and Technology of the Russian Federation, Particle Physics and Astronomy Research Council (United Kingdom), the Department of Energy (US), and the National Science Foundation (US). In addition, individual support has been received from the Swiss National Foundation, the A. P. Sloan Foundation, the Research Corporation, and the Alexander von Humboldt Foundation. The visiting groups wish to thank SLAC for the support and kind hospitality extended to them.

References

[1] I. I. Bigi, Nuovo Cim. **109 A**, 713 (1996).

[2] M. Neubert and C. T. Sachrajda, Nucl. Phys. B **483**, 339 (1997).

[3] Particle Data Group, D. E. Groom *et al.*, Eur. Phys. Jour. C **15**, 1 (2000).

[4] *BABAR* Collaboration, B. Aubert *et al.*, "The first year of the *BABAR* experiment at PEP-II", *BABAR*-CONF-00/17, submitted to the XXXth International Conference on High Energy Physics, Osaka, Japan.

[5] P. F. Harrison and H. R. Quinn, eds., "The *BABAR* physics book", SLAC-R-405 (1998), section 11.3.

[6] *BABAR* Collaboration, B. Aubert *et al.*, "Exclusive B decays to charmonium final states", *BABAR*-CONF-00/05, submitted to the XXXth International Conference on High Energy Physics, Osaka, Japan.

[7] ARGUS collaboration, H. Albrecht *et al.*, Z Phys. **C48**, 543 (1990).

[8] T. Skwarnicki, "A Study of the Radiative Cascade Transitions between the Upsilon-Prime and Upsilon Resonances", DESY F31-86-02 (thesis, unpublished) (1986).